Surface structure of γ-Fe_2O_3(111)

Michael Bowker,[1*] Graham Hutchings,[1] Philip R. Davies,[1] Dyfan Edwards,[1] Robert Davies, [1] Shamil Shaikhutdinov[2] and Hans-Joachim Freund[2]

[1]Wolfson Nanoscience Laboratory and Cardiff Catalysis Institute, School of Chemistry, Cardiff University, Cardiff CF10 3AT

[2]Chemical Physics Group, Fritz Haber Institute, Faradayweg, Berlin

Abstract

The surface structure of γ-Fe_2O_3(111) has been investigated with a range of surface techniques. Two different surface structures were discovered depending upon surface preparation techniques. Sputtering followed by annealing in vacuum produced a reduced surface characterised by a (2×2) LEED pattern, whereas sputtering followed by annealing in $1x10^{-6}$ mbar oxygen produced a surface characterised by a (√3×√3)-R30° LEED pattern. The latter appears to be a very low conductivity surface, whereas the former has the band gap expected for maghemite (~2.0 eV). We propose that the reduced surface is a magnetite-like layer, whereas the oxidised surface is an Fe_2O_3-like layer.

Keywords. Iron oxide surfaces, maghemite, γ Fe_2O3, STM, ISS, LEED

Introduction

Iron oxides are an important class of materials with applications in fields ranging from construction to magnetic devices from sensors to heterogeneous catalysis. A number of important reactions take place in the presence of an iron oxide-based catalyst. These include the production of styrene from ethyl benzene [1] gold supported on iron oxide for the oxidation of CO at low temperature [2] and mixed oxide catalysts with Mo used for the selective oxidation of methanol to formaldehyde [3-6]. Notwithstanding the technological importance of iron oxide, there is relatively little work in the literature on bulk iron oxide single crystal surfaces, and in this paper we report the first study of the surface structure of maghemite, γ-Fe_2O_3.

Iron oxide exists in several phases, with haematite (α-Fe_2O_3) and magnetite (Fe_3O_4) being by far the most widely-reported as these are the principle ores of iron. Here, however, we are interested in the behaviour of maghemite, γ-Fe_2O_3, a much more rarely-investigated material in surface science, but nonetheless an important technological material widely used in magnetic storage devices. Hence it is important to begin to investigate the surface properties of this material.

Studies of the surface structures of various iron oxide phases are not trivial because multiple stable surface structures may exist [7-16]. Early LEED and XPS investigations of α-Fe_2O_3(0001) relate the surface structure to the annealing temperature. An initial LEED pattern corresponding to a p(2×2) was found upon vacuum annealing to 700 °C, but this changes to a ($\sqrt{3}\times\sqrt{3}$)-R30° structure after further annealing to 820 °C [7, 8]. The subsequent study adapted an iron oxide phase diagram to rationalise the transformations observed on an α-Fe_2O_3(0001) single crystal [8]. LEED patterns similar to those seen in other work were observed by Condon et al. [11], with a more complex surface structure becoming apparent at higher temperature and when annealing in partial pressures of O_2. Initially, sputtering left the surface disordered and reduced, requiring long annealing periods in the presence of O_2 to achieve a bulk oxide-like stoichiometry. The first LEED-characterised layer to form was Fe_3O_4(111) after annealing up to 775 °C, followed by a $Fe_{1-x}O$(111)/α-Fe_2O_3(0001) interface with a complex LEED pattern.

Some studies have shown the significant benefits of using STM to probe iron oxide surfaces, notably Wiesendanger et al. who achieved atomic level imaging on Fe_3O_4 [10]. STM of various terminating structures on an α-Fe_2O_3(0001) single crystal were first reported by Condon et al. Annealing their sample to 1000K produced an epitaxial Fe_3O_4(111) layer comprising two coexisting terminations separated by steps. One termination was identified as a ¼ monolayer of O atoms on top of ¾ monolayer of Fe atoms, whereas the second consisted of a ½ monolayer of Fe atoms overlaying a close-packed O layer in agreement with previous work [11-13]. However, upon annealing to 1100K in 1×10^{-6} mbar O_2 a biphase ordering [13] was observed. STM revealed two different structures coexisting as islands on the surface, identified as α-Fe_2O_3(0001) and $Fe_{1-x}O$(111). The long range order of the islands resulted in a superlattice believed to be responsible for the floretted LEED pattern which was seen.

A study on the (110) face of an Fe_3O_4 single crystal revealed a well ordered structure upon sputtering and annealing to 1200 K. Subsequently the surface underwent a reconstruction showing no comparable resemblance to known iron oxide phases [14].

In parallel with the work above there has been considerable effort devoted to making thin layer model iron oxide surfaces, and this has been thoroughly reviewed by Weiss and Ranke [16]. In general thin layer oxides display similar structural behaviour to the bulk crystals described above, but give the capability of switching

surface structures/phases between FeO-like, Fe_2O_3-like and Fe_3O_4-like forms, depending on the exact details of oxidation treatment. However, it may be that the electronic structure of very thin films is different from that of the bulk crystal, and any exposed underlying Pt (used as the support) may have significant effects on, for instance, their reactive behaviour. Thus it is important to compare such materials with bulk oxides, such as the single crystal iron oxide work reported here and in the papers cited above, especially so since it is not clear that γ-Fe_2O_3 has actually been produced in thin film form [16].

In our laboratories we are engaged in studies of the structure and reactivity of both thin film iron oxides and bulk iron oxide single crystals [17,18]. In this case we are dealing with an example of the latter. As noted above, there is relatively little surface science work in the literature on bulk iron oxide single crystals, and nothing on γ-Fe_2O_3. We are particularly interested in the inter-relationships between the surface structure of the various iron oxides, and in how the surface structure relates to surface reactivity. The iron oxide phase maghemite (γ-Fe_2O_3), which is the subject of this investigation, has similarities to both magnetite and haematite - it is isostructural with the former, that is, it is a spinel ferrite, and exhibits ferrimagnetism, and yet is fully oxidised like the latter and so contains no Fe^{2+}. Thus it is an inherently interesting material, but to our knowledge there have been no surface science studies of bulk single crystal maghemite, and hence the main aim of this work was to investigate the surface structure of this material in a well-defined, single crystal form.

Experimental

The experiments were carried out on two pieces of equipment: a small ultra high vacuum (UHV I), and a custom-designed Omicron Multiprobe UHV system (UHV II). UHV I comprises a stainless steel chamber maintaining a base pressure of ~5×10^{-10} mbar equipped with an ISIS ion gun for sample cleaning, an OCI system for low energy electron diffraction (LEED) and Auger electron spectroscopy (AES), and a Hiden quadrupole mass spectrometer. The naturally grown γ-Fe_2O_3(111) crystal (from Surface Preparation Laboratory, Netherlands) was mounted on a holder which was attached directly onto the system's manipulator. Heating was achieved radiatively via W wire coils situated underneath the sample holder. The temperature was recorded through a thermocouple spot welded onto the sample holder in direct contact with the sample. For oxygen annealing, the gas was dosed via a leak valve through a stainless steel dosing tube, directed at the sample.

UHV II consists of four UHV chambers pumped by three turbo pumps and four ion pumps, giving a typical base pressure of ~1×10^{-9} mbar. The preparation chamber (P) comprises a fast entry lock and an Omicron ISE ion gun for sputtering. The analysis (A) chamber is equipped with Omicron SpectaLEED apparatus, a twin anode x-ray source for x-ray photoelectron spectroscopy (XPS), an Omicron ISE ion gun for ion scattering spectroscopy (ISS) and an energy analyser used with both XPS and ISS. IS spectra were recorded using an Omicron ISE 100 fine focus ion gun at an ion beam current of 1μA, and an energy of 1keV at a He pressure of 10 -7 mbar. Adjacent to the preparation chamber, there is the SPM chamber which houses an Omicron variable temperature surface probe microscope (VT-SPM) which is used predominantly for scanning tunnelling microscopy (STM) and has a base pressure of < 10^{-10} mbar when isolated from the rest of the system by a gate valve. The γ-Fe_2O_3(111) crystal (10 mm x 10 mm x 1 mm) was mounted on a standard Omicron sample holder which could be securely transferred between the chambers using three horizontal manipulators and a linear horizontal probe. Sample heating can be achieved

on any of the three manipulators using a resistive heating filament. The temperature was recorded through a thermocouple attached to the manipulator in close proximity to the sample. Oxygen was dosed via a stainless steel dosing tube during annealing. The surface was cleaned by cycles of Ar^+ ion bombardment (1 keV, 20 min) followed by annealing either in vacuum (873K, 20min) or in oxygen (1×10^{-7} mbar, 873 K, 20 min). XP spectra were recorded with an Al Kα photon source at a pass energy of 50 eV unless stated otherwise. Binding energies were calibrated to the clean O(1s) peak for the (2x2) surface at 530.0 eV, the value reported for magnetite elsewhere [19], but the reproducibility of XPS spectra is ±0.2 eV.

Results

LEED and Auger

Two different surface terminations of the crystal were obtained, depending on the annealing conditions. When cleaned by Ar ion bombardment and annealed in vacuum for 20 min at 873 K, a hexagonal (2x2) structure was found (fig 1a) which gave an AES O_{KLL}/Fe_{L3M23V} peak to peak ratio of 4.1(fig 2). Note that in our notation, the (1x1) pattern refers to the O-sub lattice forming close-packed layers common to the iron oxide (111) surfaces. However, when the sample was annealed in oxygen (1×10^{-6} mbar) for 20 min at 873 K a (√3×√3)-R30° LEED pattern (fig 1b) was obtained, in which the spots are surrounded by hexagonally-arranged spots of lower intensity, of the type described elsewhere as 'floretting'[8, 9, 12, 20]; this is discussed in more detail below. The Auger ratio increased, but only marginally within experimental uncertainty, to 4.4 (fig 2). Note that once one structure was formed it could not be changed to the other by vacuum or oxygen annealing. It is not unreasonable to think that, in view of the treatment conditions, the (√3×√3) -R30° is the more oxidised termination of the two surface structures.

X-ray photoelectron spectroscopy (XPS)

XP spectra from the (2x2) termination are shown in fig. 3b and reveal O(1s) and Fe($2p_{3/2}$) binding energies of 530.0 eV and 710.8 eV respectively, characteristic values for iron oxide. After sputtering (fig 3a) the broadening of the spectra to lower binding energies and significant intensity at down to 706 eV are indicative of the presence of lower oxidation states (Fe^{2+}, Fe^0) with 707 eV being characteristic of Fe^0. This shows that the surface region of the crystal after annealing is mostly, if not all, Fe^{3+}.

The (√3×√3)-R30° structure, however, suffered from charging effects, which manifested as a splitting of the O(1s) and Fe(2p) peaks, this charging resulted in rather variable spectra, which are therefore not shown here. Such effects made unambiguous identification of the valence state of the iron impossible for this structure using our XPS system , though a charge compensation system would help in this respect.

Ion scattering spectroscopy (ISS)

Ion scattering spectra (fig. 4) were obtained for both surface terminations. They show an O/Fe peak ratio of 0.24±0.02 for the (2x2) surface (R_{2x2}), and 0.40±0.02 for the (√3×√3) -R30° termination ($R_{(\sqrt{3}\times\sqrt{3})}$), indicating a greater oxygen concentration in the very topmost layer of the (√3×√3)-R30° surface.

Scanning Tunnelling Microscopy (STM)

We attempted to obtain STM images from the two surfaces, but this proved very difficult. We did obtain some poor quality images for the (2x2) structure, some of which showed evidence of atomic resolution (fig 5). The interatomic distance was found to be ca. 0.58 (±0.2) nm, the same spacing found at magnetite single crystal surfaces [11] and thin films [16], as well as Fe_3O_4 surface terminations of haematite [9]. It proved impossible to get images from the $(\sqrt{3}\times\sqrt{3})$-R30° structure however, as a tunnelling current could not be found. This low conductivity, as with the charging effects seen in the XPS, suggests the surface is an insulator. An I-V curve for the (2x2) termination is shown in the inset of figure 4, which is indicative of a semiconductor, with a bandgap of ~ 2.0 eV, close to that expected for Fe_2O_3 (maghemite and haematite are similar), but much larger than that for magnetite (0.14 eV), thus confirming that the bulk material is Fe_2O_3. The fact that it was difficult to obtain STS and images for the oxidised surface indicates a much less conductive surface layer.

Discussion

Two different surface terminations have been found on the γ-Fe_2O_3 single crystal, which can be obtained by simple treatments under mild conditions in UHV. One, the (2x2), is a somewhat reduced surface prepared by sputtering the sample and annealing in vacuum; the other, the $(\sqrt{3} \times \sqrt{3})$R30º is a more oxidised surface prepared by sputtering the sample and annealing in oxygen.

The results accumulated from AES indicate that the difference in oxygen concentration in the surface *region* between the vacuum annealed and oxygen annealed surfaces is quite small. In contrast, a bigger difference in oxygen content is shown by the surface layer sensitive ISS technique, implying a very different oxygen level in the top layer. Furthermore, both the STM and XPS data suggest that the oxygen difference is sufficient to alter the conductivity of the surface, a fundamental property. These findings indicate that the structural differences are not limited solely to the surface termination, but point to structural changes within the surface and sub-surface region of γ-Fe_2O_3. Indeed, during the entire investigation, we were not able to transform one structure into the other by simply varying the annealing conditions. Once a (2x2) or $(\sqrt{3}\times\sqrt{3})$-R30° termination was formed, the only way to then form the other was by sputtering and annealing under the appropriate conditions. This is somewhat different to the results of Condon et al. [9] on an α-Fe_2O_3 crystal, where they were able to transform a (2x2) termination into a $(\sqrt{3}\times\sqrt{3})$ -R30° by annealing in oxygen at 900 K. Another important difference between the crystals was that Condon et al. observed a (2x2) structure when annealed in 10^{-6} mbar oxygen at 900 K. It was only when this surface was annealed above 1000 K that evidence of a $(\sqrt{3}\times\sqrt{3})$ -R30° structure was found, but this is dangerously close to the bulk phase transition temperature under vacuum conditions. It is possible that under more extreme oxidising/reducing or temperature conditions, the surface of our γ-Fe_2O_3 crystal might be flipped between the (2x2) and $(\sqrt{3}\times\sqrt{3})$ -R30° structures. On the other hand the differences may simply be due to the two different bulk structures.

It should be noted that the XRD patterns from γ-Fe_2O_3 and Fe_3O_4 are essentially identical (maghemite PDF no. 00-004-0755, magnetite PDF no. 01-082-1533) because the bulk structures are so similar, with the space group Fd3m. They are both spinel ferrites, with the only difference being the lack of Fe(II) in maghemite, and the presence of cation vacancies at some of the octahedral sites. Maghemite itself differs from magnetite in a number of ways. It obviously comprises no Fe^{2+} cations,

but it is not simply magnetite minus FeO, as the change in stoichiometry might imply. While the stoichiometry of magnetite is AB_2O_4, where A are tetrahedral sites and B octahedral, maghemite is represented in a number of ways in the literature but it can be considered to be $Fe_8A(Fe_{40/3}V_{8/3})B\ O_{32}$, where V represents cation vacancy sites in the basic magnetite structure lattice, and indicates that, for a perfectly ordered crystal, $1/6^{th}$ of the octahedral cation sites are vacant. Like magnetite, maghemite is also ferrimagnetic, but as noted above, has a larger band-gap of 2 eV. The structure basically consists of two types of Fe layers sandwiched between close-packed oxygen layers. One layer interleaves the oxygen layers as a layer of octahedral Fe cations (the 'Kagomé' layer), whereas the other layer is a triple layer (the mixed trigonal layer) [16]. It contains two layers of tetrahedral Fe adjacent to each oxygen layer and in between these is another layer of octahedral Fe. The structure has been described in detail elsewhere [11, 16]

Considering the √3 structure, we assume that the surface is formed by cleaving the cationic layers and ignore the possibility of reconstruction. Following Tasker's rule that polar oxide surfaces will be unstable [21] then clearly we should leave half of the charge on each cleaved surface for charge neutrality. We might expect the surface stoichiometry to be different for maghemite compared with magnetite, that is, a top layer of cations with half the Fe should be formed on symmetrically equivalent division at the cationic layers. Figure 6a shows a possible termination which gives the √3 structure. Here the cations are all on three-fold bridge sites AND the stoichiometry is correct, and is easily envisaged as a rearrangement of the octahedral-only Kagomé layer, eliminating defects to form an ordered structure. This surface then looks very much like the expected spacing for an α-Fe_2O_3 surface (0.50 nm). It is worth noting, however, that the spots in the LEED pattern of this structure are of the so-called 'floretted' type, which is also reported by Condon et al. for α-Fe_2O_3 [9, 20] and by others [8,12] and are described as due to a 'biphasic' surface in which the floretting is due to the presence of a mixed FeO-like and Fe_2O_3 surface, spatially separated, as observed in STM. Thus our surface here may be of such a type, or may be due to multiple diffraction of an underlayer through an overlayer, as suggested elsewhere [8,12]. Without STM images of this surface however, it is difficult to go any further with this identification.

It is somewhat more difficult to envisage the (2x2) termination in these terms, since it is symmetrically impossible for this to have the 3:1 O:Fe top layer stoichiometry. None of the (2x2) structures shown in figs 6b-e represent a symmetric division of the interface. It is to be noted that only the (2x2) has been seen in LEED for magnetite (111) films [16] and crystals [11], under vacuum conditions, including in recent work in this lab [22]. However, there are problems with these structures in terms of stoichiometry. For the trigonal layer shown by Weiss and Ranke [16], we have an effective surface stoichiometry of 1:4, while for the Kagomé layer it is 3:4, both of which are problematic in terms of charge balance and symmetric division of the interface; we will return to this below. Further all of the structures in fig 6 b-e could, in principle, show the hexagonal STM image of (2x2) symmetry, due to the varying height of individual atomic components. However, the ISS helps us in this respect, since the (2x2) has a lower O:Fe ratio ($R_{(2x2)}$) than the √3 structure ($R_{(\sqrt{3}\times\sqrt{3})}$), as might be expected from the different treatments to make these structures. This would appear to eliminate the trigonal structure in fig. 6d since this has a higher oxygen level than the √3. It is also unlikely to terminate as shown in fig 6b, since this would represent a highly polar surface, leaving 6c and e as possibilities; these have $R_{(2x2)}$ values of 2 and 1.33 respectively, compared with $R_{(\sqrt{3}\times\sqrt{3})}$, which is 3. These

configurations are then also closer to the expected surface stoichiometry than the other structures. Note that the termination in c is that suggested by Lennie et al. to be the most likely structure for a bulk Fe_3O_4(111) surface [11] on stability grounds and it gives the correct O:Fe ratio in ISS, and so we believe their model for the bulk magnetite termination is the same structure as the vacuum-annealed surface here.

Of course, all of this discussion has ignored the very real possibility of surface reconstruction, a phenomenon which is important in some oxides, especially when terminating in high energy planes. By way of example, we showed that thin layer BaO on Pt(111) reconstructs to nano-pyramids exposing surfaces of the lowest energy (100) plane [23]. However, we have no direct evidence of reconstruction here and certainly the overlayer structures have the expected hexagonal symmetry and spacing.

From the considerations above, then, we propose that the structure of the oxidised surface is α-Fe_2O_3 like, whilst the reduced (2x2) structure is an Fe_3O_4-like termination. The two different LEED patterns are consistent with α-Fe_2O_3 and Fe_3O_4 thin films grown on Pt(111), as well as α-Fe_2O_3 and Fe_3O_4 single crystals ([11-18]) The interatomic distance of ~0.58 nm measured by STM on the (2x2) termination is also consistent with the literature for Fe_3O_4 [9,11,16] and matches the interatomic distance we ourselves recently measured on a magnetite bulk crystal surface using the same STM [21]. The spacing for the (√3 x √3)R30º corr esponds with the spacing of ~0.50 nm that is expected for haematite [16]. These assignments then also fit with the ISS spectra, since the √3 structure has a higher $R_{(\sqrt{3}\times\sqrt{3}}$ per unit cell (3:1), than does the (2x2) proposed here (2:1 for the structure in fig 6c, and 1.33 for that in 6e), The ISS O:Fe ratio between the two surfaces (that is $R_{\sqrt{3}\times\sqrt{3}}$:$R_{2x2}$) is actually 1.7(±0.2) (see ISS results section above), close to the expected value of 1.5 for the ratio of 6f and 6c, but not so close to that of fig 6f and 6e (ratio 2.3). These structural assignments are however somewhat tentative at this stage, and so further studies of the single crystal γ-Fe_2O_3 structure by a variety of methods, especially by atomic resolution AFM, would be very useful.

Conclusions

We have investigated the surface properties of γ-Fe_2O_3 and have identified two different surface terminations. One the them is formed by vacuum annealing and has a (2x2) surface mesh, while the other, formed by oxidative treatment, has a (√3 x √3)R30° mesh. The former appears to be a somewhat reduced surface and, by comparison with work on other iron oxide surfaces, seems to be magnetite-like. The (√3 x √3) is more oxidised and is α-Fe_2O_3-like. There are significant differences in the surface conductivities of the materials, and it proved very difficult to obtain data for the (√3 x √3) using STM and XPS.

Acknowledgements. We are grateful to EPSRC for funding for DE (EP/E03974X/1) and to the Welsh Livery Fund for support for a visit to FHI by RD.

References

1. H. Pichler, *Advances in Catalysis* vol 4, Academic Press, New York (1952), p. 271.

2. M. Haruta, S. Tsubota, T. Kobayashi, H. Kageyama, M.J. Genet, B. Delmon, J. Catal. 144 (1993) 175.

3. A. P. V. Soares, M.F. Portela, A. Kiennemann, Catal. Rev.Sci. Eng., 47(2004) 125.

4. M. Bowker, R. Holroyd, A. Elliott, A. Alouche, C. Entwistle and A. Toerncrona, Catal. Letts, 83(2002)165.

5. M. P. House, A. F. Carley, M. Bowker, J. Catal., 252(2007)88.

6. M. P. House, A. F. Carley, R. Echeverria-Valda, M. Bowker, J. Phys. Chem.C, 112(2008)4333.

7. R.L. Kurtz, V.E. Henrich, Surf. Sci. 129 (1983) 345.

8. R.J. Lad, V.E. Henrich, Surf. Sci. 193 (1988) 81.

9. N.G. Condon, F.M. Leibsle, A.R. Lennie, P.W. Murray, T.M. Parker, D.J. Vaughan, G. Thornton, Surf. Sci. 397(1998)278.

10. R. Wiesendanger, I.V. Shvets, D. Burgler, G. Tarrach, H-J. Guntherodt, J.M.D. Coey, S. Graser, Science 255(1992)583.

11. A.R. Lennie, N.G. Condon, F.M. Leibsle, P.W. Murray, G. Thornton, D.J. Vaughan, Phys. Rev. B 53(1996)10244.

12. A. Barbieri, W. Weiss, M.A. Van Hove, G.A. Somorjai, Surf Sci. 302(1994)259.

13. N.G. Condon, F.M. Leibsle, A.R. Lennie, P.W. Murray, D.J. Vaughan, G. Thornton, Phys. Rev. Lett. 75(1995)1961.

14. R. Jansen, V.A.M. Brabers, H. van Kempen, Surf. Sci. 328(1995)237.

15. S. Shaikhutdinov and W. Weiss, Surf. Sci. Lett. 432(1999) L627.

16. W. Weiss and W. Ranke, Progr. Surface Sci., 70(2002)1 and references therein.

17. J.J. Uhlrich, J. Sainio, Y. Lei, D. Edwards, R. Davies, M. Bowker, S. Shaikhutdinov, H.-J. Freund, Surface Science 605 (2011) 1550.

18. R. Davies, D. Edwards, J. Gräfe, L. Gilbert, P.R. Davies, G.J. Hutchings, M. Bowker, Surface Sci., 605(2011)1754.

19. “Practical Surface Analysis” 2nd edtn, (eds. D. Briggs and M. Seah, Wiley, Chichester, 1883) Vol 1, p. 599.

20. N. G. Condon, F.M. Leibsle, A. R. Lennie, P. W. Murray, D. J. Vaughan, and G. Thornton. Phys. Rev. Letts., 75(1995)1961

21. P.W. Tasker, J. Phys. C: Solid State Phys. 12(1979)4977.

22. C. Bamroongwongdee, PhD thesis, Cardiff University, 2010.

23. M. Bowker, P.Stone, R. Smith, E. Fourre, M. Ishii and N. H. de Leeuw, Surface Sci., 600(2006)1973.

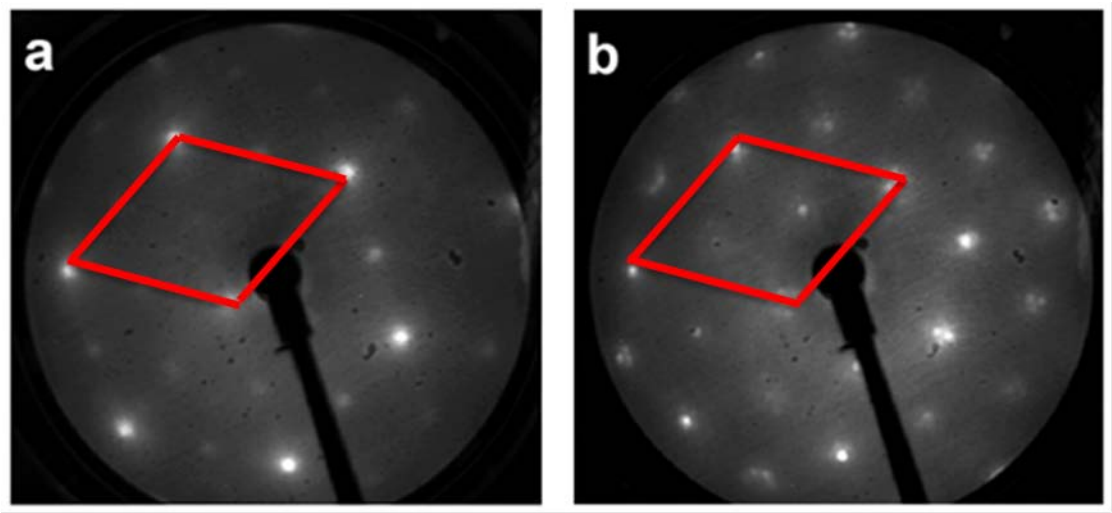

Figure 1 100 eV LEED patterns of the surface after: (a) sputtering and annealing in vacuum; (b) sputtering and annealing in oxygen. The unit cell of the O(1x1) sub-lattice common for both structures is indicated.

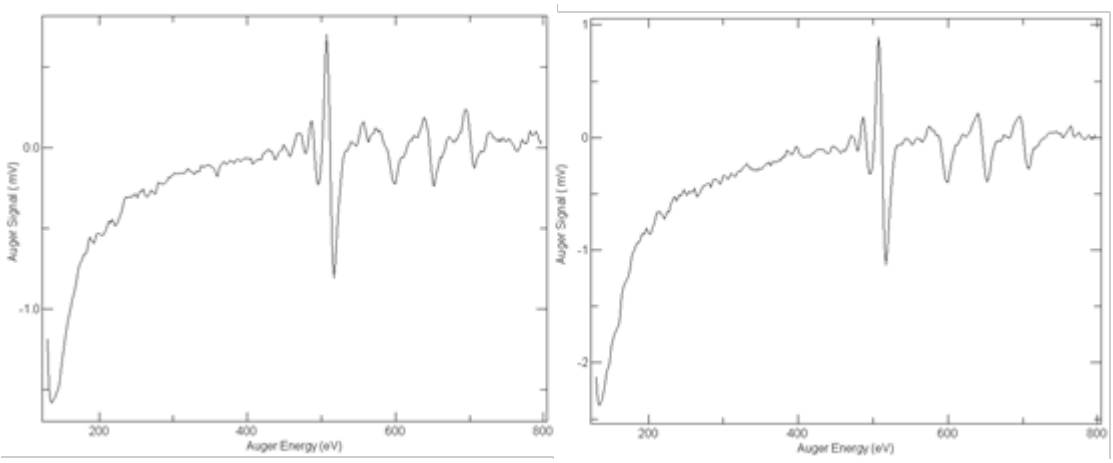

Figure 2 (a) Auger spectrum of the surface after sputtering and annealing in vacuum; (b) Auger spectrum of the surface after sputtering and annealing in oxygen.

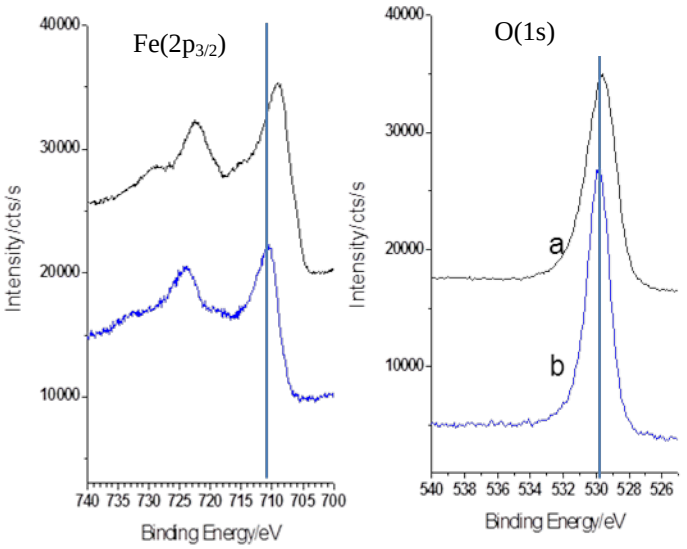

Figure 3 XPS of the γ-Fe_2O_3(111) surface, left panel Fe($2p_{3/2}$), right panel O(1s). The upper spectra (a) are for the sputtered surface and the lower spectra (b) are for the surface subsequently annealed in vacuum at 773 K for 15 minutes.

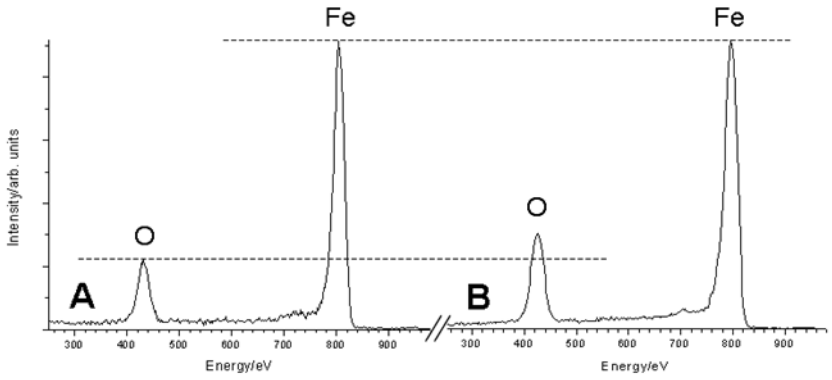

Figure 4. ISS of the iron oxide surface: (A) the sputtered and vacuum annealed (2x2), (B) the sputtered and oxygen annealed (√3 x √3)R30º, normalised to the Fe peak height.

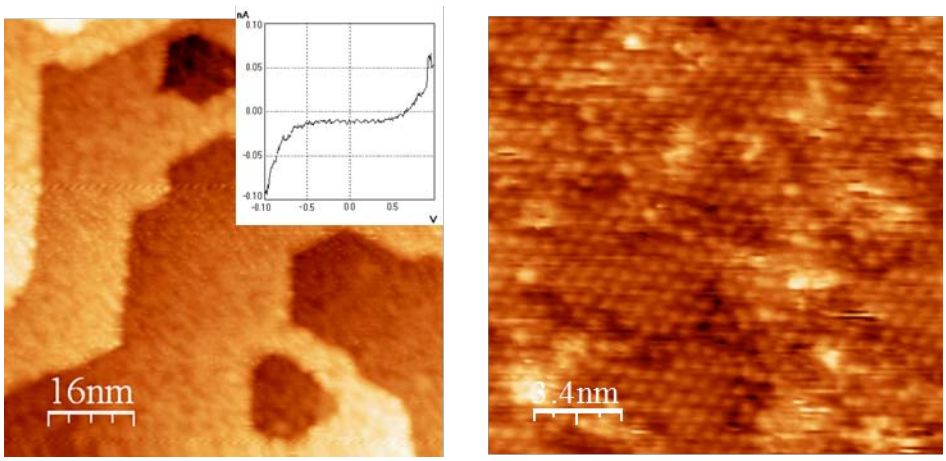

Figure 5 STM images of the (2x2) termination formed by annealing in vacuum, the inset shows the I-V curve for this surface. Image sizes are 80 x 80 nm (left panel) and 20 x 20 nm (right panel)

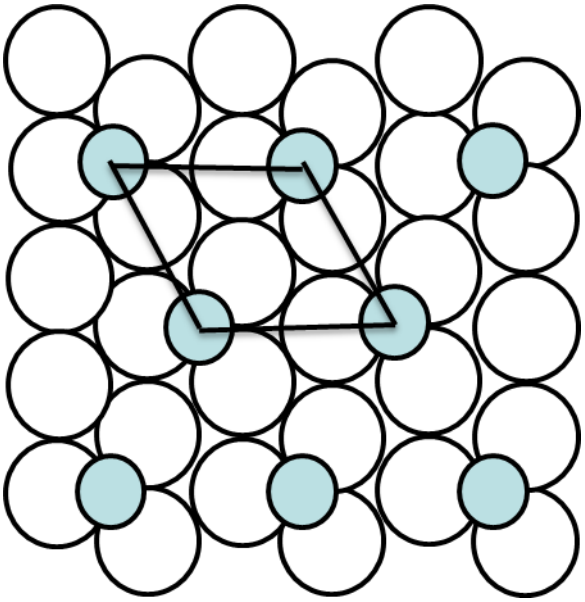

Figure 6a. The (√3 x√3)-R30° surface structure

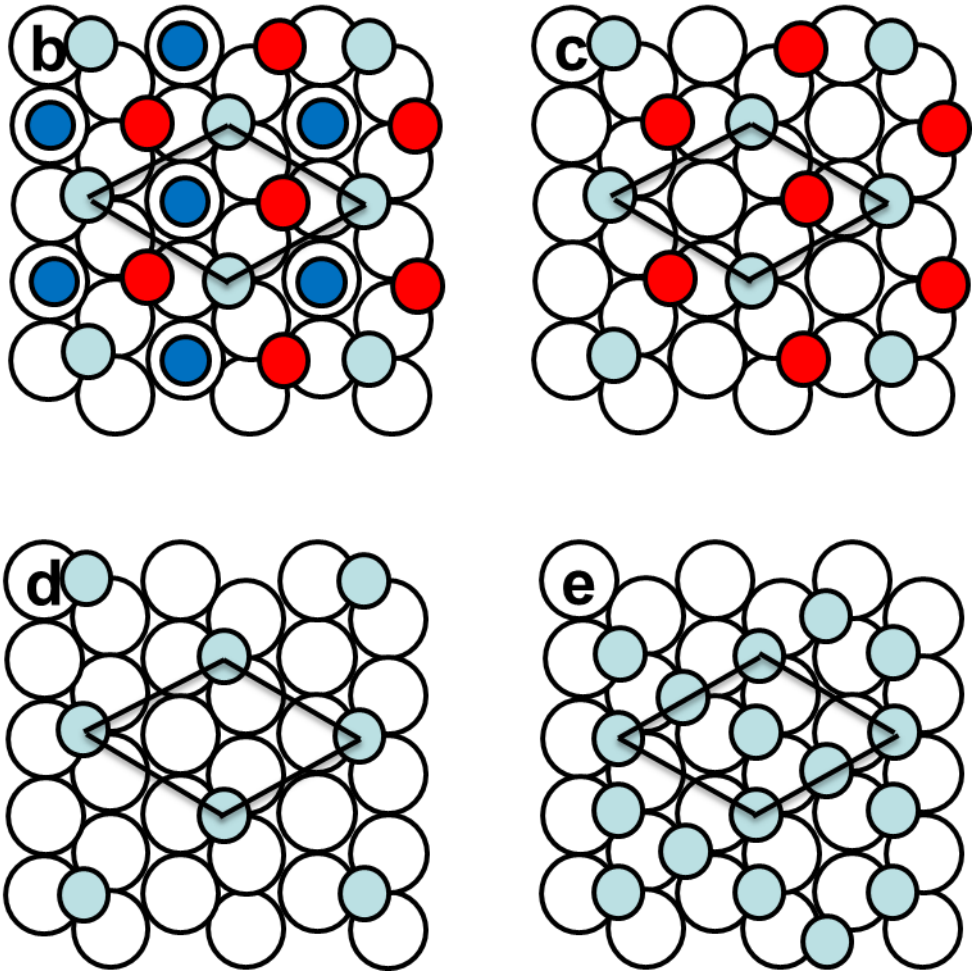

Figure 6b-e. A variety of (2x2) structures. (b) The full mixed trigonal layer of cations projected onto the surface anion layer. Large open circles are oxygen, light blue filled circles are the octahedral layer, while the red are the lower tetrahedral sites and dark blue are upper tetrahedral; (c) layer b with the upper tetrahedral layer removed; (d) layer b with both tetrahedral Fe cations removed; (e) the Kagomé structure.